02

Localized excitons in ZnMnO

© V.I. Sokolov[1], N.B. Gruzdev[1], V.V. Men'shenin[1], A.S. Vokhmintsev[2], S.S. Savchenko[2], I.A. Weinstein[2], G.A. Emelchenko[3]

[1] M.N. Mikheev Institute of Metal Physics, Ural Branch, Russian Academy of Sciences, 620108 Yekaterinburg, Russia
[2] Ural Federal University after the first President of Russia B.N. Yeltsin, 620002 Yekaterinburg, Russia
[3] Institute of Solid State Physics, Russian Academy of Sciences, 142432 Chernogolovka, Moscow oblast, Russia

e-mail: visokolov@imp.uran.ru

Received June 22, 2022
Revised August 1, 2022
Accepted August 1, 2022

Lines a, b, c, d and impurity absorption edge of ZnMnO for σ- and π-polarizations of light in temperature interval of 7−300 K were registered in this paper. Intensive lines a_π and a_σ are clearly observed in interval of 7−100 K, while other lines are observed only at low temperatures. For determination of type of optical transitions, to which excitonic lines a, b, c, d are corresponding the calculation of oscillator strength of most intensive lines was made. Lines a_π and a_σ have Lorentz form, parameters of this form were calculated with OriginPro 9.1 program. The energy of impurity absorption edge was determined. Lines a, b, c and d were analyzed in model of $Mn^{2+}-4O^{2-}$ cluster. Optical transitions take place from antibonding $(p+d^5)^*$-states in forbidden gap to state, which is splitted from the bottom of conduction band of ZnMnO. Electron-hole pairs which are localized inside the cluster are called as local excitons.

Keywords: zinc oxide, localized excitons, antibonding states.

DOI: 10.21883/EOS.2022.12.55239.3850-22

Introduction

Impurities of 3d-metals in semiconductors II−VI are actively investigated in order to create new materials for applied problems in magnetism, photoluminescence, photochemistry. The ZnMnO single crystal is of particular interest because of the significant difference in its optical properties compared to other materials II−VI:Mn. There are no absorption and luminescence bands in the optical spectrum of ZnMnO single crystals due to intracenter d^5 transitions, but there is a wide intense impurity absorption band in the energy range of $2.1-3.3$ eV, registered for the first time at room temperature in [1]. The detected band was interpreted by the authors as a result of transitions with charge transfer from the top of the valence band to the impurity center: $d^5+\hbar\omega \rightarrow d^6+h$. Recently, narrow lines a, b, c, d were found in single crystals of ZnMnO below the edge of a wide light absorption band in energy range of 1.877−1.936 eV at temperatures 4.2 and 77.3 K [2,3]. This has led to a change in the understanding of the energy states of ZnMnO. The Mn^{2+} ion creates a state in the valence band, and hybrid antibonding states $(p+d^5)^*$ exist in the ZnMnO band gap (the asterisk symbolizes the antibonding state), in which oxygen plays the main role. Optical transitions from the p states of oxygen ions O^{2-} to the conduction band under the influence of light form a wide intense impurity absorption band. The oxygen ion is positively charged relative to the lattice. The lines a, b, c, d were treated as excitons of the donor type $[(d^5+h)e]$ arising as a result of Coulomb binding of a free s-electron and a hole localized on hybridized states $(p+d^5)^*$. In the present work, the lines a, b, c, d and the edge of a wide impurity absorption band were observed in the temperature range 7−300,K, a detailed analysis of the antibonding states in the forbidden gap was carried out to identify the properties of these lines. It is shown that transitions from these states under the influence of light occur to a state split off from the bottom of the conduction band. As a result of the transitions, localized excitons are formed within the $Mn^{2+}-4O^{2-}$ cluster.

Experiment description

Low-temperature measurements of optical absorption (OA) spectra in polarized light were carried out using an installation based on a Shimadzu UV-2450 spectrophotometer and a closed-loop helium cryostat JanisCCS-100/204N. The temperature of the sample was controlled by a LakeShore Model 335 controller equipped with a diode cryogenic sensor DT-670B-CU. The vacuum inside the cryostat was created by the HiCube 80 Eco turbopump station and maintained during measurements at the level of $< 7\cdot10^{-5}$ mbar. A polarizing prism was additionally installed in the optical path of the spectrophotometer after the monochromator. The measurements were carried out at fixed temperatures: 7 K, in the range of 10−100 K in

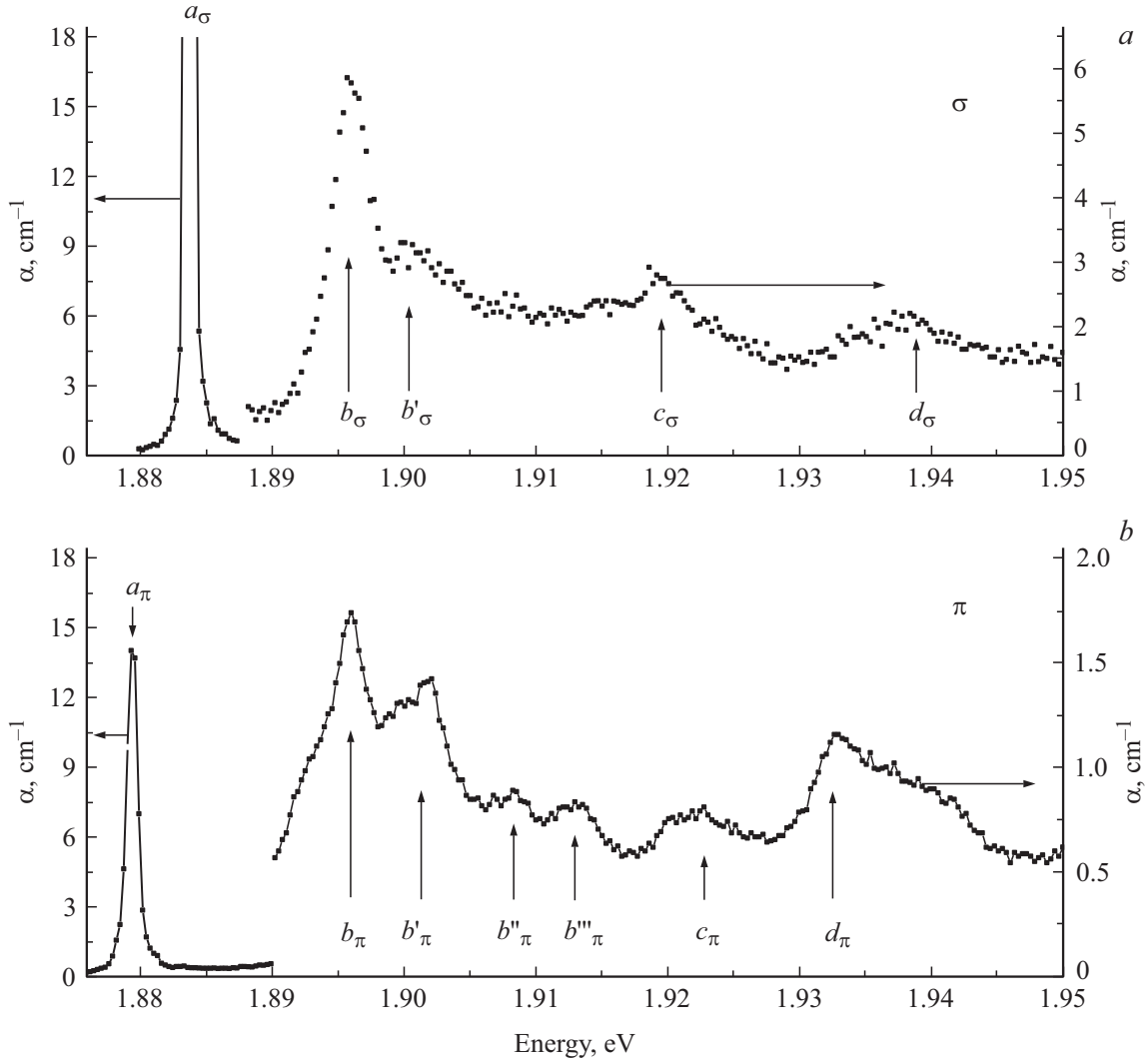

Figure 1. Optical absorption spectra of $Zn_{0.9991}Mn_{0.0009}O$ in the region of localized exciton lines for σ- and π-polarizations at $T = 7$ K.

increments of 10 K and in the range of 100–300 K in increments of 20 K. Registration of OA spectra was carried out with the following settings of the spectrophotometer: spectral range of the study — 600–700 nm; spectral width of the monochromator slit — 0.1 nm, which corresponds to 0.285 MeV or 2.3 cm^{-1}; scanning step — 0.1 nm; scanning rate — 18 nm/min. The propagation of light through the sample is shown in Fig. 1 from the work [2], the sample dimensions are indicated in the work [3]. The thickness of the sample in the direction of light propagation 0.35 cm was chosen in order to detect weak lines.

Results and discussion

Fig. 1 shows the spectra of OA $Zn_{0.9991}Mn_{0.0009}O$ in the energy range 1.875–1.950 eV at a temperature of 7 K. The intensities of the peaks of σ-polarization exceed the intensities of the peaks of π-polarization, which corresponds to the results of the work [3]. The maximum of the a_σ line is not registered due to the fact that the intensity of the light after the sample falls below the sensitivity limit of the optical system. This is due to the thickness of the sample and the relatively high absorption coefficient of the line a_σ. The appearance of new weak lines b'_σ for σ-polarization, b''_π and b''_π for π-polarization is clearly visible, which is undoubtedly due to the better resolution of the Shimadzu UV spectrophotometer-2450 as compared to the optical system used in [3].

Fig. 2 shows the spectra of the σ- and π-polarization lines for temperatures of 7, 20, 70 and 100 K. With an increase in temperature from 7 to 20 K the line a_π practically does not change, and the maximum of the line a_σ at 20 K is not yet registered. At a temperature of 70 K, the lines a_π and a_σ are clearly observed, the lines b, c, d are observed for σ-polarization and practically are not observed for π-polarization. At 100 K, only the lines a_π and a_σ are preserved, and in the area of the lines b, c, d, a weak

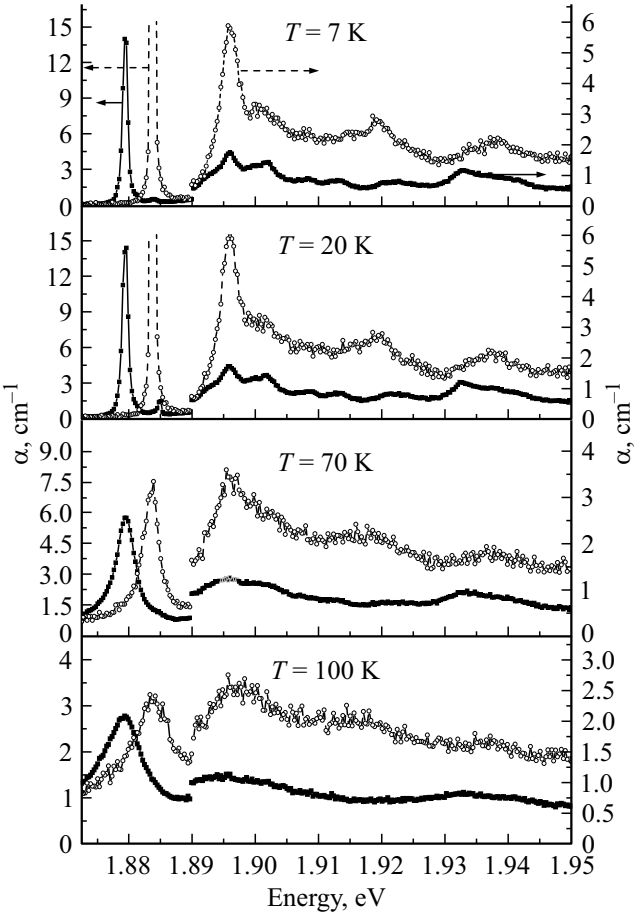

Figure 2. Spectra of $Zn_{0.9991}Mn_{0.0009}O$ OA in the region of exciton lines at different temperatures for π-polarization (dark symbols) and σ-polarization (light symbols).

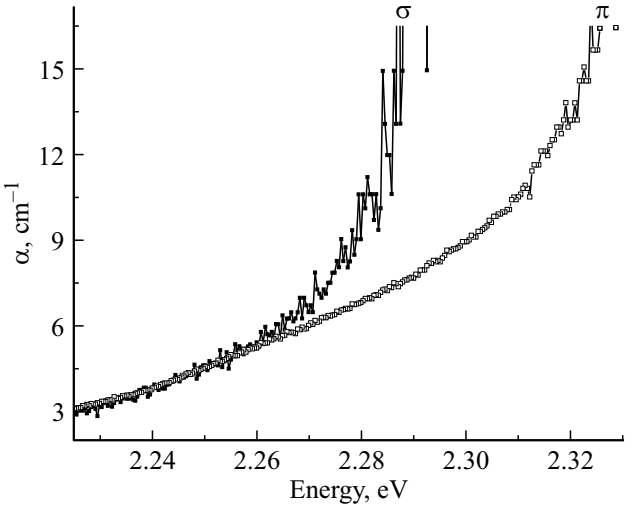

Figure 3. The OA spectra $Zn_{0.9991}Mn_{0.0009}O$ in the region of the edge of the impurity absorption band at $T = 7$ K for σ- and π-polarization.

background is observed, more intense for σ-polarization. Fig. 2 clearly shows that the ratio of the intensity maxima of the lines a_σ and s_π decreases during the transition from 70 to 100 K. This indicates that the temperature has a stronger effect on the a_σ line compared to the a_π line. The energy positions of all observed lines practically do not change with an increase in temperature to 100 K.

Fig. 3 shows the OA spectra in the region of the edge of a wide intense absorption band at temperatures 7 K for σ- and π-polarizations. Spectral curves are represented only up to a certain value of the absorption coefficient, similar to the line a_σ.

The single crystal ZnO has a symmetry group C_{6v}. When replacing a part of zinc ions with manganese, the symmetry of the $Mn^{2+}-4O^{2-}$ cluster is lowered to C_{3v}. The antibonding states of Mn^{2+} ions and O^{2-} ions in the forbidden gap ZnMnO will be described for the $Mn^{2+}-4\ O^{2-}$ cluster according to the scheme presented in [4]. In a cluster with symmetry C_{3v} σ- and π-oxygen molecular orbitals are described by irreducible representations $4a_1 + 4e$. The two one-dimensional representations of a_1 correspond to the molecular orbitals σ_1 and $\sigma_2 + \sigma_3 + \sigma_4$, respectively. The other two representations of a_1 have basis functions built on π-orbitals: $\pi_x = \pi_{2x} + \pi_{3x} + \pi_{4x}$ and $\pi_y = \pi_{2y} + \pi_{3y} + \pi_{4y}$.

The ground state of the Mn^{2+} ion is described by the term ^6S. Orbital $^6a_1$ with the configuration of $(a_1\uparrow)(e_1\uparrow)^2(e_2\uparrow)^2$ corresponds to orbital S in C_{3v} group in the case of an average crystal field. The group antibonding orbitals $p-d$ are written as follows: $a_1^1 = (\sigma_1 +^6 a_1)^*$, $a_1^2 = ((\sigma_2 + \sigma_3 + \sigma_4) +^6 a_1)^*$, $a_1^3 = (\pi_x + \pi_y +^6 a_1)^*$, $a_1^4 = (\pi_x - \pi_y +^6 a_1)^*$. Asterisks symbolize antibonding states. Fig. 4 shows a part of the group orbitals of the symmetric state $^6a_1$ of the $Mn^{2+}d^5$-configuration and a_1 of the molecular orbitals of the p-states oxygen ion O^{2-}. We believe that the observed lines are caused by transitions from antibonding hybridized $(p-d)^*$ states in the forbidden gap to a state split off from the bottom of the conduction band as a result of substitution of zinc ions with manganese ions (Fig. 4).

Transitions from group orbitals occur to the state a_1, which occurs due to splitting from the bottom of the conduction band of the level by an impurity of Mn. Such states are described by the Koster–Sleter model [5]. Therefore, the following matrix elements are different from zero:

$$\int d^3r \Psi'^*_{e_2}(M_-, -M_+)^T \Psi_{a_1},$$

for magnetic transitions from the energy level corresponding to MO Ψ_{a_1} to the split level at which the electron is described by the wave function Ψ'_{e_2}, which is the basis function of the representation e_2 of the group C_{3v}. In the last equality $\mathbf{M} = (-\alpha_{\mathrm{TC}})(\mathbf{L} + 2\mathbf{S})$, $\mathbf{L}$ — total orbital moment, $\mathbf{S}$ — total spin moment of ligands $2, 3, 4$, $alpha_{\mathrm{TC}}$ — fine structure constant. The value $(M_-, -M_+)^T$ is a matrix-column of basic functions $M_- = M_x - iM_y$, $-M_+ = -(M_x + iM_y)$ of an irreducible representation e of a group C_{3v}. It is easy to show that the representation of e^2 contains a unit representation, which provides a non-zero value of the

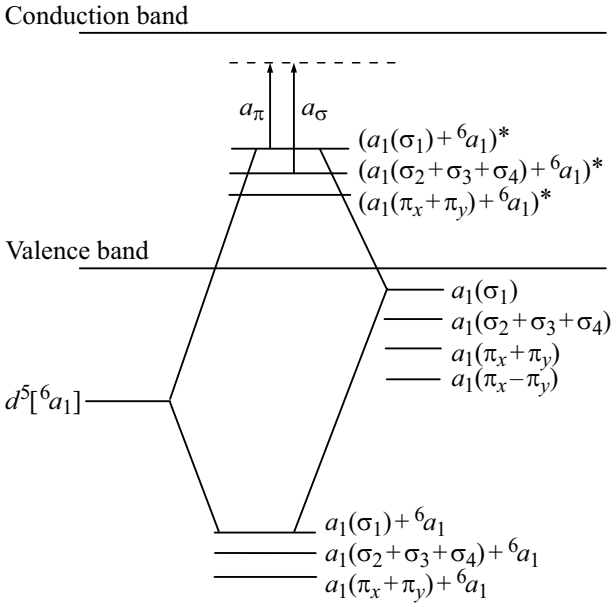

Figure 4. Approximate arrangement of antibonding hybridized $(p+d)^*$-states in the ZnMnO compound. A part of the optical transitions from the antibonding $(p+d)^*$-states to the split-off state is shown.

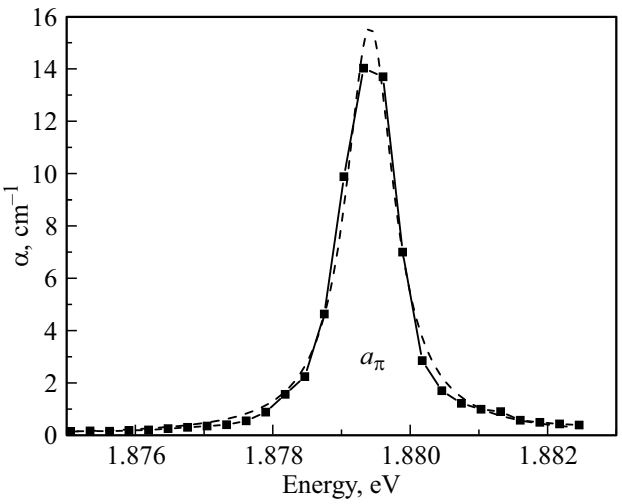

Figure 5. The OA spectrum $Zn_{0.9991}Mn_{0.0009}O$ for π-polarization at $T = 7$ K in the region of line a_π (solid curve) and its Lorentz approximation (dashed curve).

written integral. It is possible, however, to choose a simpler matrix element of the magnetic transition:

$$\int d^3r\Psi^*_{e_1}(M_-, -M_+)^T\sigma_1 = \int d^3r\{-\pi_{1y}M_+ + \pi_{1x}M_-\}\sigma_1.$$

Here the moment M refers to the first ligand. The matrix elements considered above, by replacing the magnetic basis functions with the basic coordinate spatial functions x, y, admit the existence of an electrodipole transition. However, the found oscillator forces are small for the existence of such a transition. This means that the transition of the electron to the split level from the oxygen ion is magnetodipolar.

Fig. 4 shows several antibonding states, transitions from which give the specified absorption lines. The initial states were selected so that transitions from them to the state a_1 reflected the ratio of the intensities of the observed lines. Optical transitions from group hybrids involving σorbitals are more intense compared to transitions from group hybrids involving loosely coupled πorbitals. The a_σ line originating from three σorbitals surpasses the a_π line originating from one σ orbital. Weak lines originate from π hybrids. With increasing temperature, weakly bound π-hybrids are destroyed by the thermal movement of ions in the first place. Strongly coupled σ hybrids with a large overlap of wave functions are more stable and break down at high temperatures, which we observe for the lines a_π and a_σ.

The lines a_π and a_σ have a shape close to Lorentzian. In this work, the Origin Pro 9.1 program was used for calculating the parameters of the Lorentz line of the following form:

$$a(\hbar\omega) = \frac{C\Gamma}{(\hbar\omega - \hbar\omega_0)^2 + \left(\frac{\Gamma^2}{4}\right)}.$$

In this formula, $\hbar\omega_0$ is the position of the maximum of the Lorentz curve, and Γ is the full width of the line at half of maximum (FWHM). This program calculates these parameters, as well as the maximum of the Lorentz curve and the area under this curve A (in cm^{-1}·eV). We can judged about the nature of the transition causing a certain line in the optical absorption spectrum by the strength of the oscillator of this line [4]. The value of A allows us to determine the strength of the oscillator using the formula from the work [4]:

$$f = \frac{2mc\varepsilon_0}{\pi Ne^2}\int k(\Omega)d\Omega,$$

which coincides up to a constant factor with the value of the integral $\int k(\Omega)d\Omega$ in this formula.

The strength of the oscillator for the line a_π was calculated using this formula, as well as (for greater reliability) by the formula of Smakula–Dexter for the lines of Frenkel excitons [6], for which the values Γ and ω_0 calculated by the program were used. Fig. 5 shows, for example, the Lorentz approximation of the line a_π at a temperature of 7 K, for which the following parameter values were obtained: $\omega_0 = 1.87941$ eV, $\Gamma = 8.5732 \cdot 10^{-4}$ eV, $A = 0.02101$ eV·cm^{-1}, height $H = 15.5978$ cm^{-1}. A similar procedure was performed for this line at other temperatures. The obtained dependences of the intensity and FWHM of the line a_π from the temperature are presented in the upper part of Fig. 6. In the lower part of Fig. 6, the temperature dependences of the oscillator strength of the a_π line calculated by the formulas of Bersucker and Smakula–Dexter are shown. As can be seen from the figure, both calculation methods gave close values of the

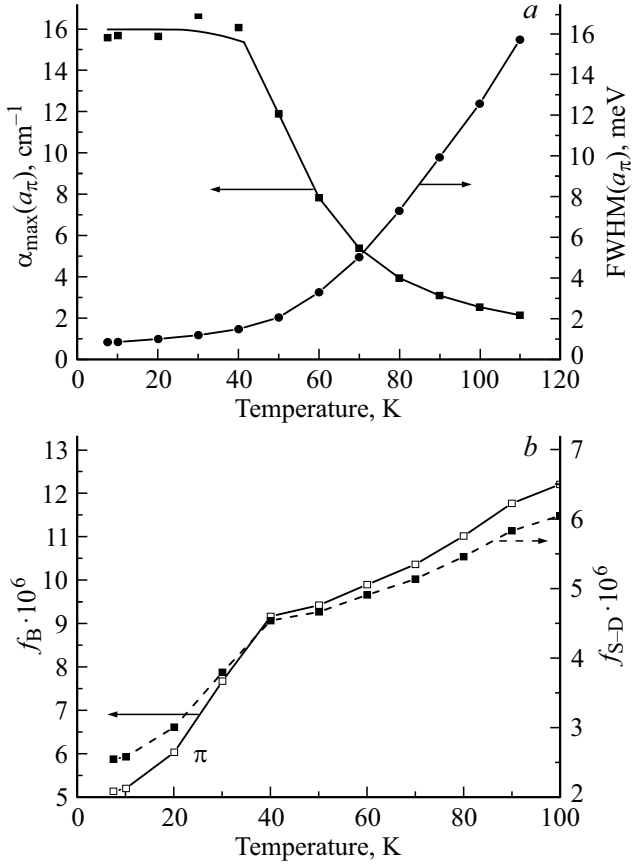

Figure 6. The dependence of the intensity and full width at half of maximum (FWHM) of the line a_π (a) and the strength of the oscillator corresponding to this line (b), from the temperature. In the figure (b), the solid curve corresponds to the oscillator forces calculated by the Bersucker formula, the dashed — to the oscillator forces calculated by the Smakula–Dexter formula.

oscillator strength. For example, at a temperature of 7 K, the following values of the oscillator strength are obtained: $f_B = 5.1 \cdot 10^{-6}$ (according to the Bersucker formula) and $f_{S\text{-}D} = 2.53 \cdot 10^{-6}$ (according to Smakula-Dexter formula), which confirms the magnetodipole nature of the a_π line discussed above. The observed increase in the strength of the oscillator with an increase in temperature is obviously associated with the broadening of the lines. The broadening of the lines, in turn, is associated with a decrease in the lifetime of exciton states in accordance with the Heisenberg uncertainty relation $\Delta E \Delta t \geq \hbar$.

As the energy of the light quanta increases, transitions to the bottom of the conduction band will begin to occur. They will form the beginning of the edge of impurity absorption. With the temperature growth, a shift of the impurity absorption edge towards lower energies is observed. Specifically, in single crystals $Zn_{1-x}Mn_xO$, the position of this edge, as our measurements show, varies slightly in the low temperature region (up to 160 K in the case of σ-polarization and up to 100 K in the case of π-polarization), and with a further increase in temperature, the dependence becomes sharper. By the position of the edge, the ionization energy E_I can be determined. To determine it, the Lukovsky formula [7] is used, obtained in the approximation of the δ-shaped potential of an impurity ion. It can be represented as

$$(\alpha d)^{(2/3}(\hbar\omega)^2 = A(\hbar\omega - E_I).$$

It is by this formula that the ionization energy was determined in this work. Fig. 7 illustrates the determination of this energy at temperatures 7 and 100,K for π-polarization. In the region of the greatest recorded absorption on the curve of the dependence of the value $(\alpha d)^{2/3}(\hbar\omega)^2$ a section was determined from the energy of the light incident on the sample, where this dependence is close to linear, then a tangent was drawn on this section, the intersection point of which with the abscissa axis corresponds exactly to the ionization energy.

Let us briefly list the new results. The lines have a small oscillator strength (10^{-6}), which is not typical for hydrogen-like states.

The energy of the impurity absorption edge is estimated in the range 2.234–2.227 eV in the temperature range 7–100 K.

The line a_π is separated by its energy position from the calculated ionization energy, which determines the edge of impurity absorption, by 356 MeV at a temperature of 7 K. This significantly exceeds the donor binding energy in ZnO, which is estimated to be approximately 75 MeV [8].

These new results do not correspond to the preliminary interpretation of the lines a, b, c, d as hydrogen-like states of the donor type $[(d^5 + h)e]$. Under the influence of light, an electron from an antibonding group orbital falls into a local state, split off from the bottom of the conduction

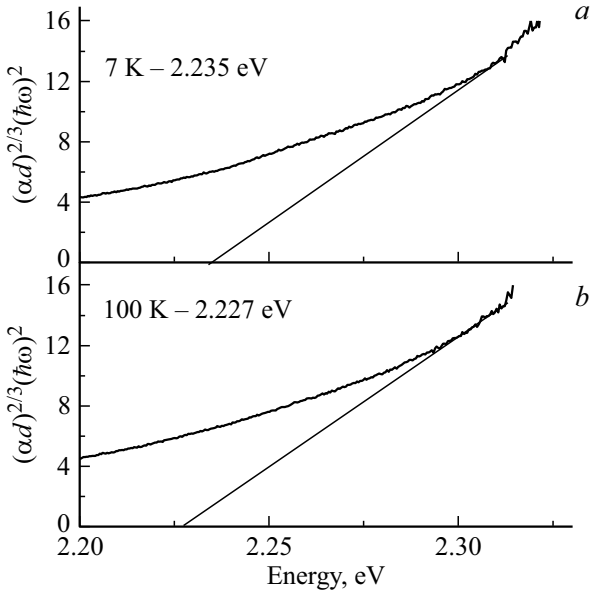

Figure 7. Determination of the ionization energy E_I by the Lukowski formula $(\alpha d)^{2/3}(\hbar\omega)^2 = A(\hbar\omega - E_I)$ for π-polarization at $T = 7$ (a) and 100 K (b).

band. The hole is also localized on oxygen ions within the $Mn^{2+}-4\ O^{2-}$ cluster. This electron-hole pair within the cluster can be considered as a localized exciton at the isovalent center. Transitions under the influence of light from different antibonding orbitals to the split state excite different localized excitons, which manifest themselves as lines of σ- and π-polarizations. Knowing the value of FWHM $8.57 \cdot 10^{-4}$ eV (Fig. 5), the lifetime of the Δt localized exciton a_π is estimated by the uncertainty ratio $\Delta E \Delta t \geq \hbar$ as $7.6 \cdot 10^{-13}$ s.

Let us briefly discuss the difference between localized excitons and donor and acceptor excitons (DE, AE) in compounds II–VI doped with impurities of $3d$ metals [9,10]. In DE and AE, the first carrier is localized in the d^n-configuration, the second — in a hydrogen-like orbit. For example, in compounds II–VI:Ni(d^8) DE and AE have the form $[d^7e]$ and $[d^9h]$, square brackets symbolize the Coulomb interaction. As a result of the formation of DE or AE under the influence of light, a significant charge change occurs on the configuration of the d^n node of the cluster, accompanied by the formation of phonons. Therefore, in the optical spectra, the DE and AE headlines have numerous vibrational repetitions, the most intense with the participation of LO-phonons [9,10]. In the case of a localized exciton in ZnMnO, vibrational repetitions are not observed. Perhaps the electron-vibrational interaction does not occur due to the absence of a significant charge change in the configuration of the d^5 cluster node.

The short lifetime of a localized exciton means that there is an effective mechanism for its relaxation. The results of the work [11] indicate that when excited into the intense absorption band Mn localized excitons a, b, c, d appear in the photoluminescence spectrum in the form of dips. There are no signs of an additional contribution to the luminescence spectrum, as it is clearly manifested for the ions Fe^{3+}. Therefore, there must be an effective mechanism of non-radiative recombination. For semiconductors with $3d$- or $4f$-impurities, nonradiative annihilation of an electron-hole pair with intracenter excitation of d^n- or f^n-configurations [12–14] has long been known. The essence of the process is that an electron-hole pair with nonradiative recombination due to Coulomb interaction can excite an electron of the impurity center. Such recombination is called Auger relaxation on the defect (DAR). An electron-hole pair can be localized on a defect, for example, as AE. The nonradiative annihilation of AE leads to the excitation of the d^n-configuration of the impurity center [13]. Or, during inter-band excitation, excitons localized on the impurity center arise, the non-radiative recombination of which excites the f center [14]. In ZnMnO, an electron-hole pair (localized exciton) arises under the influence of light in a cluster $Mn^{2+} - 4O^{2-}$. One can expect the excitation of the Mn^{2+} ion as a result of Auger relaxation. But the energies of localized excitons are approximately 1.9 eV, and the energy of the first intracenter transition of the configuration d^5 of the Mn^{2+} ion is 2.55 eV [15]. Therefore, auger relaxation does not occur. In our samples, a certain number of Fe^{3+} [3,11] ions are observed. The energy of the intracenter absorption of d^5-configurations of the Fe ion^{3+} $^6A_1 - ^4T_1$ is shifted from the energies of local excitons by less than 100 MeV. Therefore, one electron of the d^5 configuration of the Fe^{3+} ion is effectively excited. With an increase in temperature, the lifetime of localized excitons decreases (Fig. 6), which means an increase in the efficiency of the Auger process. Preliminary results on the excitation of photoluminescence of the Fe^{3+} ion, unambiguously indicating the manifestation of Auger relaxation, will be presented later.

Conclusion

Localized excitons were detected in ZnMnO. They are formed as a result of magnetodipole transitions from antibonding $p-d$ states in the forbidden gap to a state split off from the bottom of the conduction band having a low oscillator strength $(2-5) \cdot 10^{-6}$. The lifetime of such excitons is determined by the efficiency of Auger relaxation with electron excitation in the d^5-ion configuration Fe^{3+}. The interstitial variant of Auger recombination has not been observed before.

Funding

The work was carried out within the framework of the state assignment of the Ministry of Education and Science of Russia (topics „Electron“, № 122021000039-4, „Quantum“, № 122021000038-7), as well as with the financial support of the Ural Federal University Development Program within the framework of the strategic academic leadership program „Priority-2030“.

Conflict of interest

There is no conflict of interest between the authors.

References

[1] F.W. Kleinlein, R. Helbig. Z. Physik, **266**, 201 (1974).
[2] V.I. Sokolov, N.B. Gruzdev, V.A. Vazhenin, A.V. Fokin, A.V. Druzhinin. Phys. Sol. St., **61** (5), 702 (2019). DOI: 10.1134/S1063783419050354.
[3] V.I. Sokolov, N.B. Gruzdev, V.A. Vazhenin, A.V. Fokin, A.V. Korolev, V.V. Menshenin. J. Exp. Theor. Phys., **130** (5), 681 (2020). DOI: 10.1134/S1063776120040123].
[4] I.B. Bersucker. Elektronnoe stroenie i svoistva koordinatsionnykh soedinenii (Electronic structure and properties of coordination compounds) (Khimiya, Leningrad, 1976).
[5] G.F. Koster, J.C. Slater. Phys. Rev., **95**, 1167 (1954).
[6] D.L. Dexter.Phys. Rev., **101** (1), 48 (1956).
[7] G. Lucovsky. Solid State Comm., **3**, 299 (1965).
[8] H. Morkoç, A. Özgür. *Zinc Oxide* (WILEY-VCN Verlag, Weinheim, 2009).
[9] K.A. Kikoin,V.N. Fleurov. *Transition Meta lImpurities in Semiconductors* (World Sci., Singapore,1994).

[10] V.I. Sokolov, K.A. Kikoin. Soviet Scientific Rev. A, **12**, 147 (1989).
[11] V.I. Sokolov, N.B. Gruzdev, V.N. Churmanov, V.V. Menshenin, G.A. Emelchenko. Low Temperature Physics, **47** (1), 38 (2021).
[12] R.J. Robbins, P.J. Dean. Adv. Phys., **27**, 499 (1978).
[13] S.G. Bishop, R.J. Robbins, P.J. Dean. Solid State Comm., **33**, 119 (1980).
[14] G.G. Zegrya, V.F. Masterov. Phys. Techn. Semicond., **29**, 1893 (1995).
[15] T. Mizokawa, T. Nambu, A. Fujimori, T. Fukumura, M. Kawasaki. Phys. Rev. B, **65**, 085209 (2002). DOI:10.1103/PhysRevB.65.085209